Numerical Analyses of Various Sizes of Mortise and Tenon Furniture Joints

Ali Kasal,[a,*] Jerzy Smardzewski,[b] Tolga Kuşkun,[a] and Yusuf Ziya Erdil [a]

This study reports the moment resistance, stiffness, and numerical analysis of various sizes of round-end mortise and tenon joints. L-shaped and T-shaped specimens were constructed. Joints were manufactured using three tenon widths and three tenon lengths with 10 replications for each combination. Specimens were constructed of Turkish beech, and the joints were assembled with polyvinylacetate (PVAc) adhesive. Bending tests were carried out in compliance with accepted test methods. Numerical analyses were performed with finite element method (FEM) software. At the end of the study, the joints became stronger and stiffer as either tenon width or length increased. Tenon length had a more significant effect on moment resistance, while tenon width had a more significant effect on stiffness. Ultimate moment resistances were obtained with L-shaped joint construction of 50 × 50 mm tenons and T-shaped joint construction of 40 × 50 mm tenons. Strength of a chair could be increased by considering these results in engineering design process. Results showed that the numerical analyses gave reasonable estimates of mechanical behavior of joints. Analytical calculations and numerical simulations confirmed that the maximum stress in the glue line was concentrated at the edge and corners, and that the modeled joints had a shape-adhesive nature.

Keywords: Furniture joints; Mortise; Tenon; Strength; Stiffness; Finite element method

*Contact information: a: Department of Wood Science and Industrial Engineering, Faculty of Technology Mugla Sitki Kocman University, 48000 Kötekli/Mugla, Turkey; b: Faculty of Wood Technology Collegium Maximum 28 Wojska Polskiego st. 60-637 Poznan, Poland; *Corresponding author: alikasal@mu.edu.tr*

INTRODUCTION

The members that compose furniture frames are joined at the required points with different joint techniques. The strength of the joints represents the entire system of the chair frame. The joints that are the most critical parts of the furniture frames should therefore have sufficient strength. To develop a reliable system, data on joint strength, stiffness, and the features of the mechanical behavior properties should be established properly and taken into concern to improve strength.

Mortise and tenon joints have been used for thousands of years by woodworkers around the world to join pieces of wooden members, mainly when the adjoining pieces connect at an angle of 90°. They are still favored for furniture frame constructions. There are many factors that affect the moment capacity of mortise and tenon joints, including the tenon size (length, width, and thickness), type of fit, shape of the plug and hole, thickness of the glue line, wood species, and adhesives used (Smardzewski 2002; Dzincic and Skakic 2012; Dzincic and Zıvanic 2014).

Previous studies have defined several factors that affect the strength of mortise and tenon joints. The study carried out by Tankut and Tankut (2005) was undertaken to obtain the strength of round tenon/round mortise, rectangular tenon/rectangular mortise, and

rectangular tenon/round mortise joints assembled under the same conditions, with different end configurations. The results of the study showed that rectangular-end mortise and tenons were approximately 15% stronger than both round-end mortise and tenons, and rectangular-end tenons fitting into round-end mortise joints. The results also indicated that if tenon width or length increased, the strength of the joint correspondingly improved. A predictive expression was developed for rectangular mortise and tenon joints that takes into account wood species, adhesive type, and joint geometry, specifically, tenon width, tenon shoulder width, and tenon length (Erdil *et al.* 2005). The comparative bending and fatigue strength of rectangular mortise and tenon joints constructed of oil palm (*Elaeis guineensis*) lumber have also been evaluated. The results showed that the bending strength of oil palm lumber joints was half of the strength of the other wooden joints. In terms of fatigue strength, joints constructed of oil palm lumber showed comparable performance with the other wood materials. The results of the study also showed that the allowable design stresses of rectangular mortise and tenon joints could be set at 20% of their bending strength (Ratnasingam *et al.* 2010). The bending moment capacity and moment rotation characteristics of mortise and tenon joints as a function of tenon geometry, grain orientation, length, and shoulder fit were examined by Likos *et al.* (2012). The bending moment capacity for all of the joints in which tenons were fully inserted into mortises was 54% greater than that of joints in which tenons were not fully inserted. Joints with 25.4-mm-long diamond-shaped tenons had greater moment capacity than either rectangular or round tenon joints, but joints with 38- or 51-mm-long rectangular tenons had greater capacities than joints with diamond or round tenons. The effects of adhesive type and loose tenon dimensions (length and thickness) on bending strength under uniaxial bending load of T-shaped mortise and loose tenon joints were investigated by Derikvand and Ebrahimi (2014). Polyvinyl acetate (PVAc) and two-component polyurethane (PU) adhesives were used to construct joint specimens. The bending moment capacity of the joints increased significantly with increased length and thickness of the loose tenon, and the joints constructed with PU had approximately 13% higher bending moment capacity than the joints constructed with PVAc.

Kasal *et al.* (2013) researched the effect of wood species, adhesive type, and tenon width and length on the static bending moment capacity and stiffness of T-shaped round-end mortise and tenon furniture joints. The results indicated that tenon length had a more significant effect on the moment capacity of the joints than tenon width, whereas tenon width had a more significant effect on joint stiffness than tenon length. Furthermore, an empirically derived expression was developed to predict the average ultimate bending moment capacity of round-end mortise and tenon joints. In a similar study, an empirically derived expression was developed to estimate the average ultimate bending moment capacity of L-shaped round-end mortise and tenon joints under compression and tension loads as a function of wood species, adhesive type, and tenon size (Kasal *et al.* 2015a).

Moment resistance of end-to-side floating tenon joints as a function of tenon shape, geometry of the tenon surfaces, bond line thickness, tenon width, and wood species was studied by Derikvand and Eckelman (2015). The results indicated that round-edge loose tenons were 20% stronger than rectangular-edge tenons seated into round-end mortises. The degree of fit between the tenon and the inside walls of the mortise exhibited the most important effect on the bending capacity of the joints. The highest bending moment capacity was obtained in beech joints made with 45-mm-wide grooved tenons that had a glue line thickness of 0.05 mm.

With the development of technology, modern management and production techniques, integrated with mathematical optimization techniques, are quickly established in businesses. Therefore, businesses are required to catch up with the technological development by using computer and optimization techniques as a tool for maintaining their existence within the intensely competitive market (Koç *et al.* 2011).

The exact strength analysis of furniture frames is a computationally complex process because of the large number of internal forces that must be determined to reach an effective solution. Technology has developed very rapidly. As with other industrial products, the developments in technology have influenced the furniture in each phase from design to production. The use of technological developments is very important to strengthen the design of furniture. The engineering design of furniture can be accomplished by utilizing solid modeling and structural analysis software. Finite element methods (FEM) provide the most convenient tool for analyzing furniture systems. Furniture members, joints, and the entirety of the system can be modelled parametrically *via* FEM. Even though a simple change in the design phase can influence the entire system, because of the facilities provided by solid modelling, changes can be made virtually, and the modified design of the system can be compared to the original. Thus, an optimum solution can be obtained. The strength calculations of the designed members, joints, and the whole system could be made by simulating real conditions and loads to a solid modelled system, so that the stresses at the nodes or members could be obtained. Afterwards, the optimization could be provided by interpretation of these stresses. By utilizing virtual design, prototyping and research-development costs could be reduced (Kasal 2004).

Kasal and Puella (1995) developed analytical models for the structural analysis of furniture frames by finite element methods. They collected the stiffness and the load-deformation characteristics of joints experimentally, and then incorporated the results into the input for the analysis models. It was concluded that the analytical models created by finite element methods provided information on the deformations and internal forces acting on a piece of furniture in use. Gustafsson (1995, 1996, 1997) used FEM to analyze chairs constructed with some Swedish wood species. His works are worth mentioning because of his approach to the structural analysis of chairs by means of modern computer programs. Smardzewski (1998) developed a computer program designed for rigidity/strength analysis of furniture side frame constructions. The results indicated that the computer program allowed accurate, rapid, and multiple rigidity/strength analyses of furniture side frames constructed of wood.

Smardzewski and Prekrat (2009) presented a method for the dimension sub-optimization of the cross-section diameters of a sofa frame construction. They demonstrated the need for virtual prototyping of upholstered furniture in integrated computer-aided design (CAD) and computer-aided engineering (CAE) environments. The proposed dimensions of the main construction elements, put forward following the performed sub-optimization, decreased beech wood consumption by 36% and that of particleboard by 25%. Reduced dimensions of the most important construction elements did not result in a significant decrease of the stiffness and strength of the sofa frame.

Numerical analysis of the stress and strain conditions of a three-dimensional furniture skeleton construction and its joints were presented by Horman *et al.* (2010). The finite volume method was utilized in the calculations. The displacement of the edge point from the loaded joint was also determined. The results of the calculations and the experimental data were in agreement. The numerical results also provided an opportunity for identification of the region with the largest load and strain in the complex chair skeleton

construction, which is one of the most complex pieces of furniture. Another study (Horman *et al.* 2012) presented analysis of the stiffness and strength of the chair side frame, carried out by analytical and numerical methods. The force method was used in analytical consideration of the problem. In the numerical analysis, the equations for momentum balance were discretized by the finite volume technique. The accuracy of the analytical method was confirmed by comparing the calculated results with the data numerically obtained. The results showed that the stiffness and strength of the chair's side frame were affected by the position and geometric characteristics of the stretcher cross-section, which allows selection of its optimal size and position.

The study carried out by Hajdarevic and Martinovic (2014) presented numerical analyses of the effects of tenon length on the flexibility of mortise and tenon joints. Numerical calculations were carried out with the finite element method. The results of the study indicated that mortise and tenon joints became stiffer as tenon length increased. Furthermore, the results revealed that the stiffness of the joints in a frame had a considerable impact on the structure deflection. Kuşkun (2013) and Kasal *et al.* (2015b) researched the effect of tenon size on the strength of chair frame joints, along with the relations between the static and cyclic loading forms. A simple approach was developed for estimating the whole structure strength from the individual joint tests, and it was demonstrated that the cyclic performance of a chair is equivalent to 56% of the static strength. Hajdarevic and Busuladzic (2015) performed stiffness analyses of a statically indeterminate wood chair side-frame. Numerical calculations were carried out with a "linear elastic model" for orthotropic materials, and the model was solved by the finite element method. The results of the calculation indicated that the chair side frame became stiffer as the position of the stretcher lowered and/or the stretcher cross-section increased. The results revealed that the stiffness of the joints in a frame have a considerable impact on the structure deflection.

İmirzi *et al.* (2015) determined the strength, stiffness, and substitute modulus of elasticity of dowel, mortise and loose-tenon, and mortise and tenon L-type furniture joints under diagonal tension and compression loads. The specimens were constructed from Turkish beech (*Fagus orientalis* L.), white oak (*Quercus alba*), and white walnut (*Juglans cinerea* L.), and were assembled with a water-resistant PVAc adhesive. According to the results, the highest stiffness/strength values were estimated in mortise and tenon joints constructed of white oak, while dowel joints constructed from Turkish beech showed the lowest stiffness/strength and deformability. The substitute modulus of elasticity of the experimental joints was a better expression of stiffness than the stiffness coefficient. The accuracy of the developed elasticity modulus model of the examined joints was verified by experimental studies and numerical calculations.

An important amount of the chair frames manufactured in the Turkish furniture industry, particularly those produced by small manufacturers, are constructed of Turkish beech (*Fagus orientalis* L.) with mortise and tenon joints. The main purpose of this study was to obtain practical information concerning the moment resistance and stiffness of L-shaped and T-shaped joints constructed of Turkish beech using different tenon sizes. The study tested how tenon size (tenon depth and length) affects the moment resistance and stiffness of L-shaped and T-shaped joints, along with testing whether the numerical analysis, by means of the finite element method, could give reasonable estimates for L-shaped and T-shaped joints.

EXPERIMENTAL

Plan of the Study and Experimental Models

A total of 90 L-shaped joint specimens, representing the front-leg-to-side-rail joint, and 90 T-shaped joint specimens, representing the back-leg-to-side-rail joint, were constructed of Turkish beech (*Fagus orientalis* L.) with round-end mortise and tenon joints, and tested to determine their moment resistance and stiffness. The joints were constructed using nine different tenon sizes from three tenon widths (30, 40, and 50 mm) and three tenon lengths (30, 40, and 50 mm), with 10 replications of each. Full linear models (Model 1, Model 2, Model 3, and Model 4) for the two-way factorial experiments were considered to determine the effects of tenon width and tenon length on the moment resistance and stiffness of L-shaped and T-shaped joints. The models are as follows,

$$LM_{ijk} = \mu_1 + A_i + B_j + (AB)_{ij} + \varepsilon_{ijk} \quad (1)$$

$$LR_{ijk} = \mu_2 + A_i + B_j + (AB)_{ij} + \varepsilon_{ijk} \quad (2)$$

$$TM_{ijk} = \mu_1 + A_i + B_j + (AB)_{ij} + \varepsilon_{ijk} \quad (3)$$

$$TR_{ijk} = \mu_2 + A_i + B_j + (AB)_{ij} + \varepsilon_{ijk} \quad (4)$$

where LM_{ijk}, LR_{ijk}, TM_{ijk}, and TR_{ijk} refer to the moment resistance (Nm) and stiffness (N/mm) values of L- and T-shaped joints, respectively; μ_1 and μ_2 refer to the population means for the moment resistance (Nm) and stiffness (N/mm) for all tenon width-tenon length combinations, respectively; *A* refers to the discrete variable representing the effect of tenon width; *B* refers to the discrete variable representing the effect of tenon length; *(AB)* refers to the effect of the two-way interaction among the two variables; ε refers to the random error term; *i* refers to the index for tenon width, 1,...,3; *j* refers to the index for tenon length, 1,...,3; and *k* refers to the index for the replicate, 1,...,10.

Test Materials

All of the joint specimens were constructed of Turkish beech (*Fagus orientalis* L.), which is commonly used in the Turkish furniture industry. The wood materials were obtained from commercial suppliers. The average density value was 620 kg/m^3. The wood was conditioned to, and held at, approximately 12% moisture content (MC) before and during testing. Physical and mechanical properties of the wood were evaluated in accordance with the procedures described in ASTM D4442 (2001) and ASTM D1037 (2001), respectively.

The 65% solids content PVAc glue, which is widely used as assembly glue, especially for furniture frames, was utilized for assembling the joint specimens.

General Configuration and Construction of the Specimens

The L-shaped and T-shaped joint specimens consisted of two members—a leg and a rail (Fig. 1). It should be noted that in material preparation and assembly, small wood-shop techniques were utilized. All of the wood used in this study was cut from air-dried timbers by means of a band saw. First, all of the members of the joint specimens were planed on a jointer, and then they were planed to 21 mm thick on a planer. Afterwards, the widths of the members were cut into 60-mm and final length sizes.

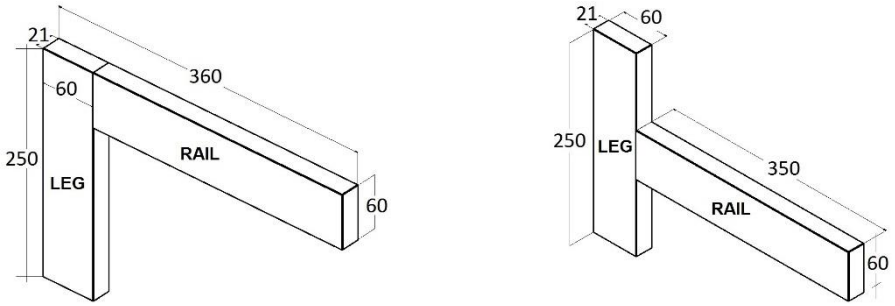

(a) (b)

Fig. 1. (a) L-shaped and (b) T-shaped specimens (measurements in mm)

Cross-sections of all of the members of the joint specimens were the same, with 21-mm thickness and 60-mm width. In the following phase, the mortises and tenons were marked in the members of the L-shaped and T-shaped joints. For the mortise and tenon joints, tenons measured 30, 40, and 50 mm width, by 30, 40, and 50 mm length, by 7 mm (1/3 of the member thickness) thick. Tenon configurations are given in Fig. 2.

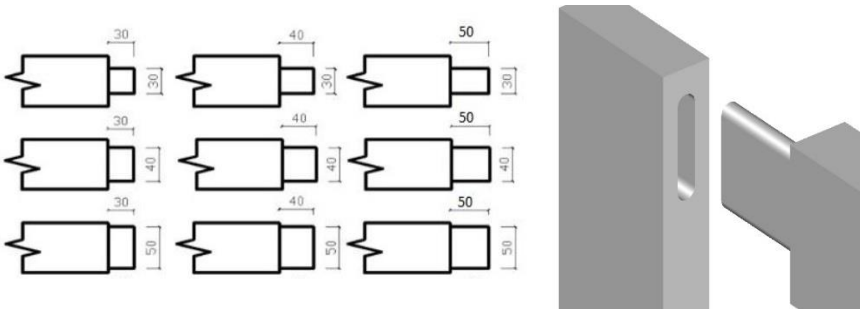

(a) (b)

Fig. 2. Geometries of (a) the various sizes of tenons and (b) detail of a round-edge mortise and tenon (measurements in mm)

A mortising machine and a tenoning machine were utilized for opening the mortises and cutting the tenons, respectively. The clearance and type of fit were not observed according to a standard or a norm. However, a snug fit (average mortise-tenon clearance of 0.076 ± 0.025 mm) was obtained between the tenons and mortises. The adhesive was liberally applied to all faces of the tenon and to the sides and bottom of the mortise. Pieces of wax paper with mortises in them to accommodate the tenons were used to prevent any possibility of the members adhering.

Before the tests, to eliminate moisture content variations, the joint specimens were allowed to cure for a minimum of one month after assembly in an environmentally controlled conditioning room that was set to produce average MC of 12%.

Methods of Loading and Testing

All of the bending tests of the L-shaped and T-shaped joints were carried out on a 50-kN capacity universal-testing machine (Mares 2007, Turkey) in the mechanical test laboratory of Wood Science and Industrial Engineering Department of Muğla Sıtkı Koçman University with a 6 mm/min loading rate under static loading. The MC specimens were cut from the specimens and weighed immediately after each test.

A concentrated load was applied to the rail member of each specimen at a point 300 mm from the front edge of the leg; *i.e.*, the moment arm was 300 mm (Fig. 3).

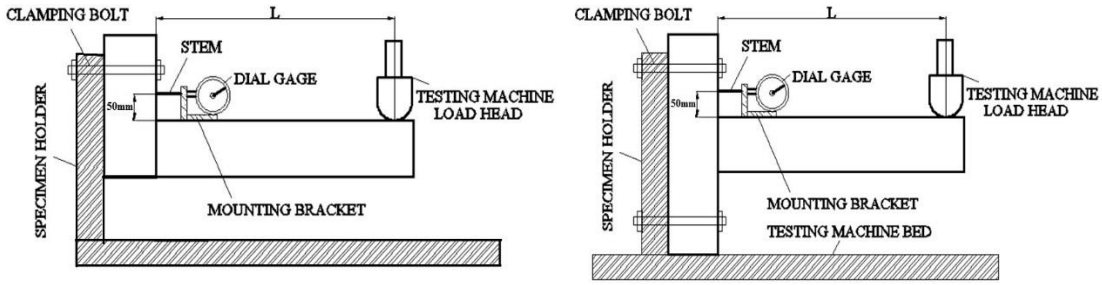

(a) (b)

Fig. 3. Diagrams showing the bending loading forms and attachments of (a) L- and (b) T-shaped joint specimens to the test rig

The loading was continued until a breakage or separation occurred in the specimens. The ultimate loads carried by the joints were recorded with a tolerance of 0.01 N. The ultimate loads were then converted to corresponding moment resistance values by means of the expression,

$$M = F \cdot L \quad (5)$$

where M refers to the moment resistance of L-shaped or T-shaped joints (Nm), F refers to the ultimate applied force (N), and L refers to the moment arm (m).

Measurements of joint stiffness were obtained by means of a dial gage clamped to the top edge of the rail for both L-shaped and T-shaped joint specimens. Dial gage readings were taken at regular intervals as the specimens were loaded.

Numerical Analyses of Mortise and Tenon Joints

Numerical calculations were performed with finite element method software (Autodesk Simulation Mechanical, 2015). The module for nonlinear analysis of orthotropic materials, including large deformations, was used. Mesh models of an L-shaped joint, along with a tenon and glue line (thickness 0.1 mm) are shown in Fig. 4.

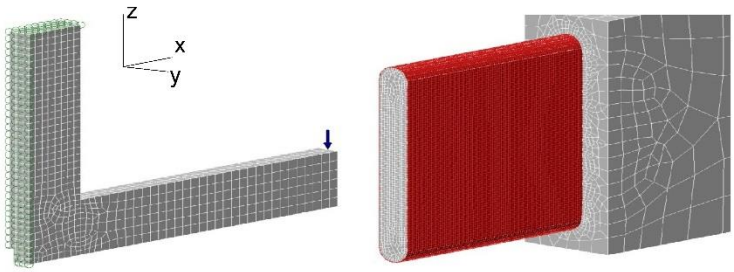

(a) (b)

Fig. 4. Mesh model of (a) an L-shaped joint and (b) glue line and tenon

In the construction of the numerical model, brick eight-node finite element modeling was used. In the case of the beech wood, a nonlinear orthotropic model of finite elements was used, while in the case of the glue line, an isotropic component was used.

Between all flat surfaces of the glue line, a mortise and tenon bonded connection was used. For others surfaces, surface-to-surface contact was modeled. The elastic properties of the materials are presented in Table 1.

Table 1. Elastic Properties of Materials Used in the Joints

Material	Modulus of Elasticity (N/mm²)			Poisson Ratio			Kirchhoff Modulus (N/mm²)		
	E_X	E_Y	E_Z	V_{XY}	V_{YZ}	V_{XZ}	G_{XY}	G_{YZ}	G_{XZ}
Turkish Beech	11553	1160	2280	0.448	0.073	0.708	470	1640	1080
PVAc Glue Line	460			0.3			177		

E_X, E_Y, E_Z: Modulus of elasticity in grain, radial, and tangential directions, respectively; V_{XY}, V_{YZ}, V_{XZ}: Poisson's ratio on grain-radial, radial-tangential, and grain-tangential planes, respectively; G_{XY}, G_{YZ}, G_{xz}: Kirchhoff Modulus on grain-radial, radial-tangential, and grain-tangential planes, respectively.

Models of the L-shaped and T-shaped joints were supported by the experimental data. External load was represented by the concentrated force, *T*. The value of this force increased as follows: 29.43, 58.86, 88.29, 117.72, 147.15, 176.58, 235.44, and 294.30 N. The displacement was recorded as a direction of force *T*. On the basis of the results of the numerical calculations, the strength and stiffness of the joints were compared for L- (Fig. 5a) and T-shaped (Fig. 5b) joints.

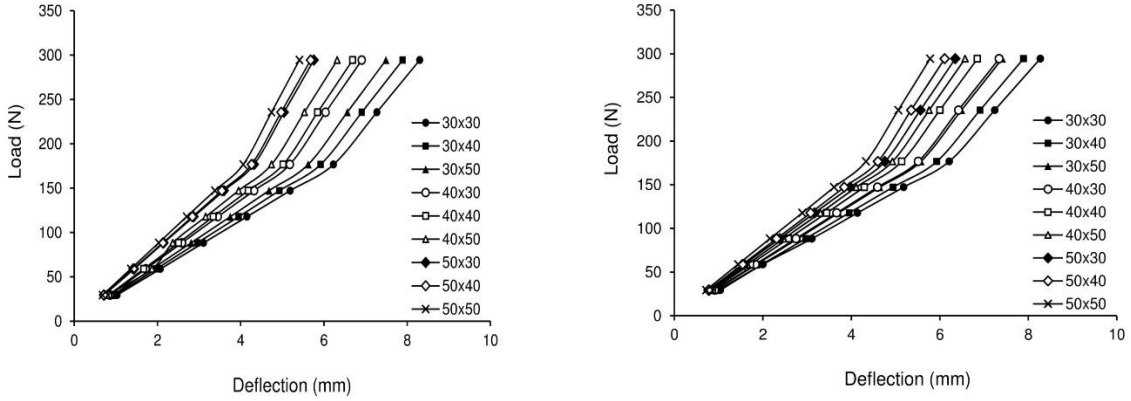

Fig. 5. Stiffness of (a) L-shaped and (b) T-shaped joints – results of numerical calculations

RESULTS AND DISCUSSION

Moment Resistance and Stiffness

Some physical and mechanical properties determined in this study are given in Table 2.

Table 2. Physical and Mechanical Properties of Beech Used in the Study

Wood Species	E* (N/mm²)	Tension Strength (N/mm²)	Compression Strength (N/mm²)	Shear Strength (N/mm²)	MOR* (N/mm²)	Density (g/cm³)	MC* (%)
Turkish Beech	11553	118.4	60.7	10.31	115.9	0.60	10.8

*E: Modulus of elasticity; MOR: Modulus of rupture; MC: Moisture content

Results of the moment resistance and stiffness of L-shaped and T-shaped joints, with their coefficients of variation, are given in Table 3.

Table 3. Mean Moment Resistance and Stiffness of L-shaped and T-Shaped Joints with Corresponding Coefficients of Variation*

Tenon Width (mm)	Tenon Length (mm)	L-shaped Joints						T-shaped Joints					
		Moment (Nm)			Stiffness (Nm/rad)			Moment (Nm)			Stiffness (Nm/rad)		
		Mean	COV (%)	HG	Mean	COV (%)	HG	Mean	COV (%)	HG	Mean	COV (%)	HG
30	30	100	5.45	D	1235	22.03	CD	104	11.35	F	1942	10.15	CD
	40	97	11.16	D	927	17.71	E	88	12.17	G	2085	21.73	CD
	50	130	11.81	C	930	16.99	E	159	5.09	D	1868	14.16	D
40	30	105	8.31	D	1193	8.59	D	107	6.34	EF	2283	24.68	BC
	40	136	8.46	C	1314	9.90	BCD	197	4.24	B	3070	14.04	A
	50	140	11.04	C	1343	11.76	ABCD	213	6.01	A	2503	14.39	B
50	30	99	14.09	D	1526	29.57	A	81	14.56	G	1913	13.47	D
	40	178	8.90	B	1420	14.16	ABC	117	4.79	E	2515	24.60	B
	50	220	4.29	A	1439	17.39	AB	170	12.58	C	3086	11.72	A

*Values followed by the same capital letter are not significantly different; COV: Coefficient of variation

In general, both L-shaped and T-shaped joints failed completely between 1 and 2 min. In the tests, joints opened up suddenly, but they kept holding the loads for a while. In the joints constructed with small-width and large-length tenons, failures occurred because of fracture of the tenons and their point of entry into the walls of the legs. In the case of small-length tenons, joints failed with glue line fracture. In other words, the short tenons withdrew completely from the leg members, so the joints were broken into pieces. In the case of large-width and large-length tenons, the common method of failure was pull-out of the tenons from the leg member, with some core wood materials attached to the tenon. Opening failures started at the edge of the joint section and then propagated toward the other edge of the joint, with increasing load for the joint. As the glue line lost its strength, the tenons started to take the load. Some splits occurred on the top of the leg member of L-shaped joints, owing to the forcing of the tenons under shear in a direction parallel to the grain.

Two-way analyses of variances (MANOVA) general linear model procedures were performed for both the moment resistance and stiffness data of the joints to analyze main effects and interaction effects on the means of moment resistance and stiffness. The MANOVA results indicated that the effects of the main factors (tenon width and tenon length) and two-factor interactions on both moment resistance and stiffness of L-shaped

and T-shaped joints were statistically significant at the 5% significance level, except for the effect of tenon length on the stiffness of L-shaped joints. The analyses of variances are given in Table 4 for L-shaped and T-shaped joints.

Table 4. Summary of the ANOVA Results for Moment Resistance and Stiffness

		Source	Degrees of Freedom	Sum of Squares	Mean Squares	F Value	Prob. (Sig)
MOMENT	L-shaped Joints	Tenon Width	2	50910.199	25455.099	167.7759	0.0000
		Tenon Length	2	58152.555	29076.278	191.6433	0.0000
		Width x Length	4	31896.360	7974.090	52.5577	0.0000
		Error	81	12289.385	151.721		
		Total	89	153248.499			
	T-shaped Joints	Tenon Width	2	55201.685	27600.843	202.5981	0.0000
		Tenon Length	2	103585.565	51792.782	380.1739	0.0000
		Width x Length	4	28526.323	7131.581	52.3479	0.0000
		Error	81	11034.990	136.234		
		Total	89	198348.563			
STIFFNESS	L-shaped Joints	Tenon Width	2	2815199.699	1407599.849	28.3408	0.0000
		Tenon Length	2	163332.155	81666.077	1.6443	0.1995
		Width x Length	4	652034.337	163008.584	3.2820	0.0152
		Error	81	4023013.134	49666.829		
		Total	89	7653579.324			
	T-shaped Joints	Tenon Width	2	7326816.119	3663408.060	21.5909	0.0000
		Tenon Length	2	4591073.247	2295536.624	13.5291	0.0000
		Width x Length	4	5833048.292	1458262.073	8.5945	0.0000
		Error	81	13743591.517	169673.969		
		Total	89	31494529.175			

The least significant difference (LSD) multiple comparison procedure was performed at the 5% significance level to determine the mean differences in moment resistance and stiffness values of the L-shaped and T-shaped joints, considering the tenon width–tenon length interaction in the MANOVA results mentioned above. In other words, mean comparisons for the two-way interactions were analyzed.

Generally, the results indicated that the moment resistance and stiffness of L-shaped and T-shaped joints increased as the tenon width or length increased. However, tenon width had a greater effect on stiffness than tenon length, while tenon length had a more significant effect on moment resistance than tenon width

Figure 6 shows the mean comparisons of moment resistance and stiffness of L-shaped and T-shaped joints for tenon width. The single LSD values were 6.328 Nm and 5.996 Nm for the moment resistance of L-shaped and T-shaped joints, respectively, and 114.5 Nm/rad and 211.6 Nm/rad for the stiffness of L-shaped and T-shaped joints, respectively. The results indicated that the moment resistance of L-shaped joints increased considerably as the tenon width increased. For L-shaped joints, increasing the tenon width from 30 mm to 40 mm increased the moment resistance approximately 16%, while an increase from 40 mm to 50 mm, increased the moment resistance approximately 31%.

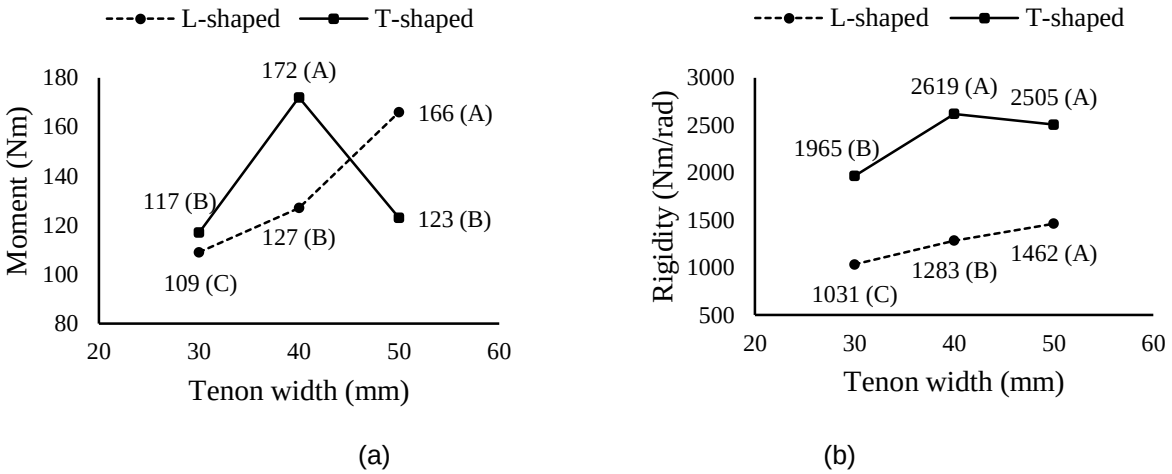

(a) (b)

Fig. 6. Mean comparisons for the effect of tenon width on the (a) moment resistance and (b) stiffness of L-shaped and T-shaped joints

In the case of the T-shaped joints, however, similar results were not obtained. There was no significant difference between 30-mm and 50-mm width tenons. However, the highest moment resistance was obtained with 40-mm width tenons. For T-shaped joints, increasing the tenon width from 30 mm to 40 mm increased the moment resistance approximately 47%, while increasing the tenon width from 40 mm to 50 mm decreased the moment resistance about 29%. As with moment resistance, the stiffness values of the L-shaped joints increased as the tenon width increased. Increasing the tenon width from 30 mm to 40 mm increased the stiffness approximately 25%, while an increase from 40 mm to 50 mm increased the stiffness by approximately 14%. Stiffness values of the T-shaped joints were similar to the T-shaped moment resistance values. The only difference between the two cases is that there was no statistically significant difference between 40-mm and 50-mm width tenons for stiffness values. However, the highest stiffness values were obtained with the 40-mm width tenons, as with moment resistance. Increasing the tenon width from 30 mm to 40 mm increased the stiffness approximately 33% for T-shaped joints. Generally, it could be said that T-shaped joints had higher stiffness values than L-shaped joints for each tenon width.

Mean moment resistance and stiffness of L-shaped and T-shaped joints, along with LSD comparison test results for tenon length, are given in Fig. 7.

The single LSD values were 6.328 Nm and 5.996 Nm for the moment resistance of L- and T-shaped joints, respectively, and 211.6 Nm/rad for the stiffness of T-shaped joints. As can be seen in Fig. 7, the moment resistance of the L-shaped and T-shaped joints increased considerably as the tenon length increased. Increasing the tenon length from 30 mm to 40 mm increased the moment resistance of the joints approximately 37% for both joint types. Increasing the tenon length from 40 mm to 50 mm increased the moment resistance approximately 19% for L-shaped joints, and approximately 35% for T-shaped joints. No significant differences were obtained between the stiffness values for 30, 40, and 50-mm length tenons for L-shaped joints. In the case of T-shaped joints, stiffness values increased as the tenon length increased, as with tenon width. Increasing the tenon length from 30 mm to 40 mm increased the stiffness approximately 25%, but there was no statistically significant difference between 40-mm and 50-mm length tenons. Increasing the tenon width from 40 mm to 50 mm decreased the stiffness approximately 3% for T-shaped joints.

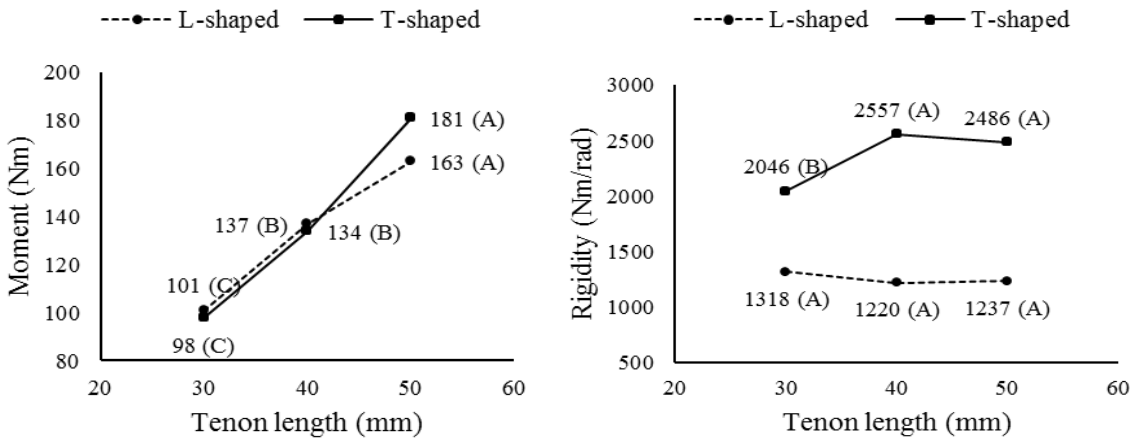

(a) (b)

Fig. 7. Mean comparisons for the effect of tenon length on the (a) moment resistance and (b) stiffness of L- and T-shaped joints

Numerical Analysis Results

Figure 8 shows the effect of the size and shape of the glue line on the tangential stress distribution in the adhesive joint.

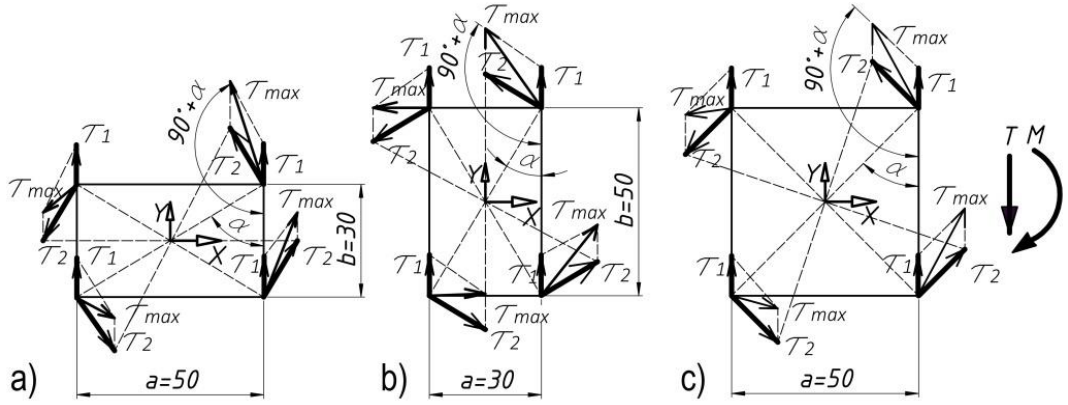

Fig. 8. Tangential stress distribution in (a) 30 × 50, (b) 50 × 30, and (c) 50 × 50 mortise and tenon joints

In the presented case, the vertical force *T* passes through the middle of the glue line, and it causes an average state of stresses, τ_1, on the entire surface of the glue line with a value of:

$$\tau_1 = \frac{T}{n\,ab} \tag{6}$$

where *a* and *b* refer to dimensions of the glue line (mm) and *n* refers to number of the glue lines.

By continuing to maintain the state of balance between the external moment $M=T\cdot L$ and the moment originating from the sum of stresses, τ_2, it was obtained:

$$M = n \cdot \tau_2 \int_A \int \sqrt{x^2 + y^2}\, dx dy \tag{7}$$

where x and y are the coordinates of stress vector in Cartesian coordinates, and *A* is the surface of glue line.

Therefore, the value of the maximum stress occurring in the corners of the glue line can be determined according to the formula,

$$\tau_2 = \frac{M}{J}\frac{\sqrt{(a/2)^2 + (b/2)^2}}{n} \quad (8)$$

where *M* refers to the maximum bending moment (Nm) and *J* refers to moment of inertia of the cross-section of the glue line in relation to the middle of rotation 0, calculated as follows:

$$J = \int_{-\frac{1}{2}b}^{\frac{1}{2}b}\int_{-\frac{1}{2}a}^{\frac{1}{2}a}(x^2 + y^2)dxdy = a \cdot b\frac{(a^2 + b^2)}{12} \quad (9)$$

Therefore, the greatest static stress is the sum of the component stresses, τ_1 and τ_2, in one of the corners of the glue line. According to Fig. 8, it amounts to:

$$\tau_{max} = \sqrt{\tau_1^2 + \tau_2^2 - 2\tau_1\tau_2\cos(90^o + \alpha)} \quad (10)$$

Table 5 shows the results of the analytical calculations of shear stresses in different types of glue lines: 30 × 50, 50 × 30, and 50 × 50.

Table 5. Value of Tangential Stresses in Different Types of Glue Lines

Parameter	Unit	Type of Glue Line		
		30 × 50	50 × 30	50 × 50
Height (*b*)	mm	30	50	50
Width (*a*)		50	30	50
Alpha (*α*)	°	59	31	45
Length of Arm (*L*)	mm	300		
Force (*T*)	N	294.3		
Moment (*M*)	Nmm	88290		
Stress (t_1)	N/mm²	0.10	0.10	0.06
Stress (t_2)		88.29	88.29	52.97
Stress (t_{max})		88.37	88.34	53.02

The maximum stress in the 30 × 50 and 50 × 30 mm joints had the same value, 88.37 N/mm^2. In the case of 50 × 50 mm joints, the maximum shear stress was 40% lower at 53.02 N/mm^2. This might suggest similar strength and stiffness of 30 × 50 and 50 × 30 mm joints, as well as a higher stiffness and strength of 50 × 50 mm joints. Similar relationships were valid between 30 × 40 and 40 × 30 mm joints.

From Fig. 5, it appears that the highest stiffness values were present in the joints with the largest length of glue line: 50 × 50, 50 × 40, and 50 × 30 mm. The lowest stiffness values were seen in 30 × 50, 30 × 40, and 30 × 30 mm joints. For the load of about 176.58 N stiffness of joint significantly increased. This change of stiffness was caused by an

increase of contact stresses between the mortise and tenon. For the same reasons, the stiffness of 50 × 30 and 40 × 30 mm joints was greater than the stiffness of 30 × 50 and 30 × 40 mm joints.

This phenomenon is illustrated in Figs. 9, 10, 11, and 12. From Fig. 9, it can be observed that the maximum value of reduced stress (30 N/mm^2) occurred in the upper part of the 50 × 30 mm mortise and tenon. In the case of the 50 × 50 mm joint, such stresses occurred on both sides of the joint, on a smaller area. Figures 10 and 11, respectively, show contact stresses on the surface of tenons and mortises. They show that the contact pressure between the mortise and tenon in 50 × 30 mm joints was much larger than in 50 × 50 mm joints. Furthermore, this pressure occurred on the upper surface of the mortise. In the case of 50 × 50 mm joints, increased pressure occurred near the front edge of the mortise. The pressure between the mortise and tenon migrated through the glue line (Fig. 12). This means that in the case of 50 × 30 mm joints, the glue line transferred contact pressure along the entire upper edge. These pressures reached a peak of 60 N/mm^2 and reduced shear stresses in the glue line.

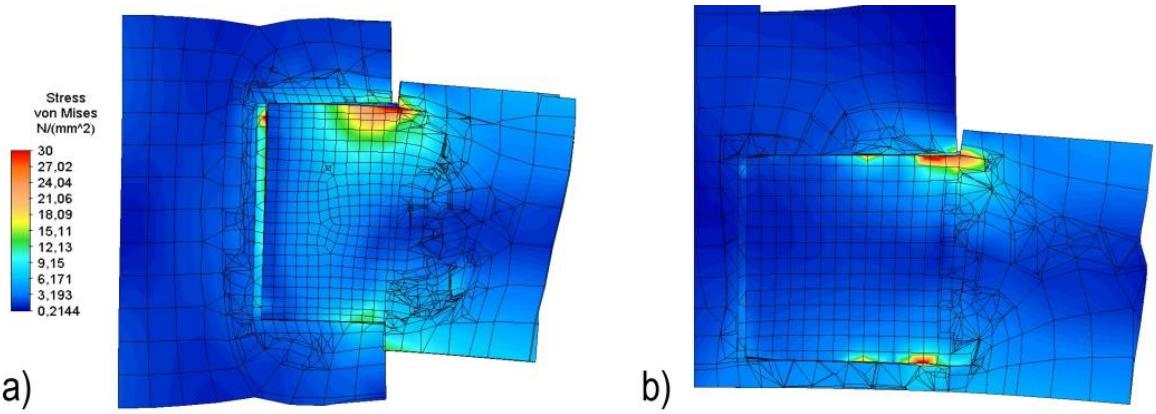

Fig. 9. Distribution of reduced stress in (a) 50 × 30 and (b) 50 × 50 mm mortise and tenon joints

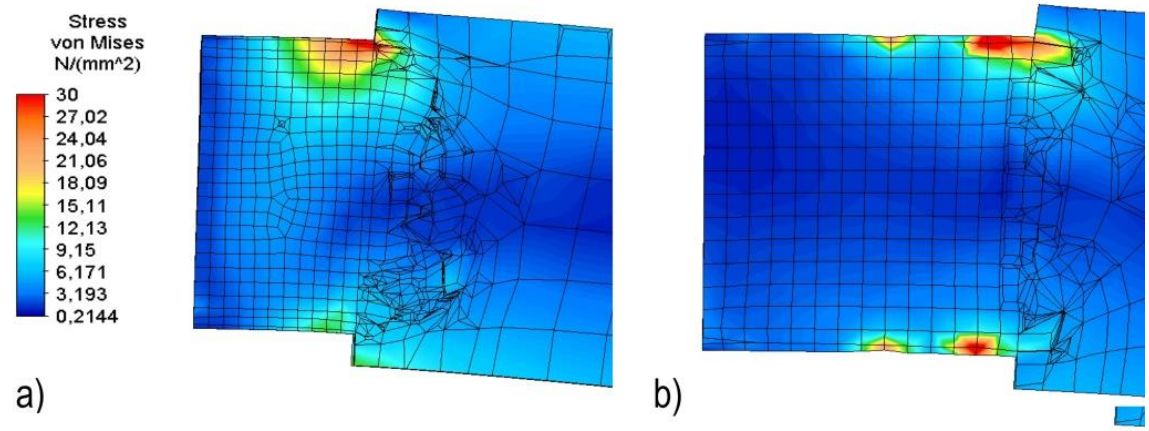

Fig. 10. Distribution of reduced stress in (a) 50 × 30 and (b) 50 × 50 mm tenons

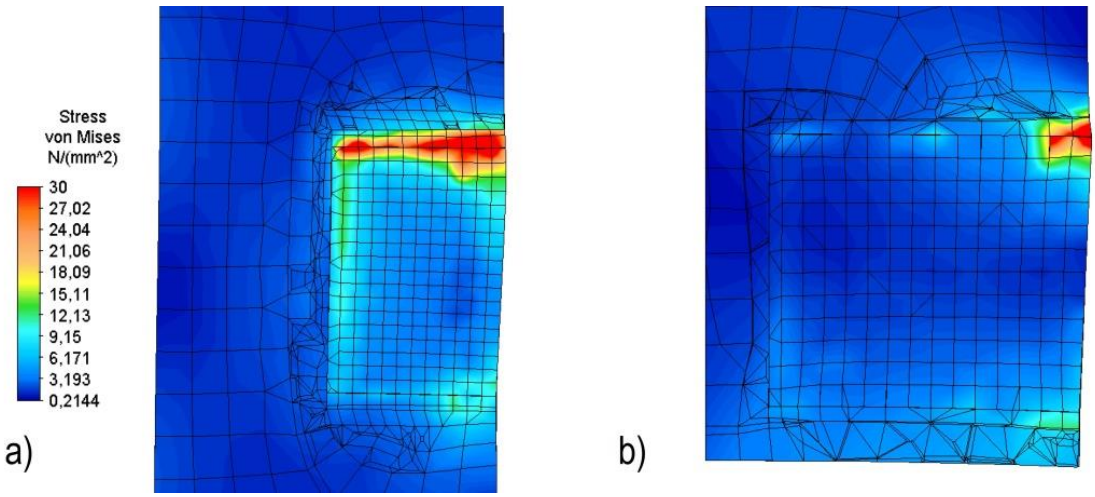

Fig. 11. Distribution of reduced stress in (a) 50 × 30 and (b) 50 × 50 mm mortises

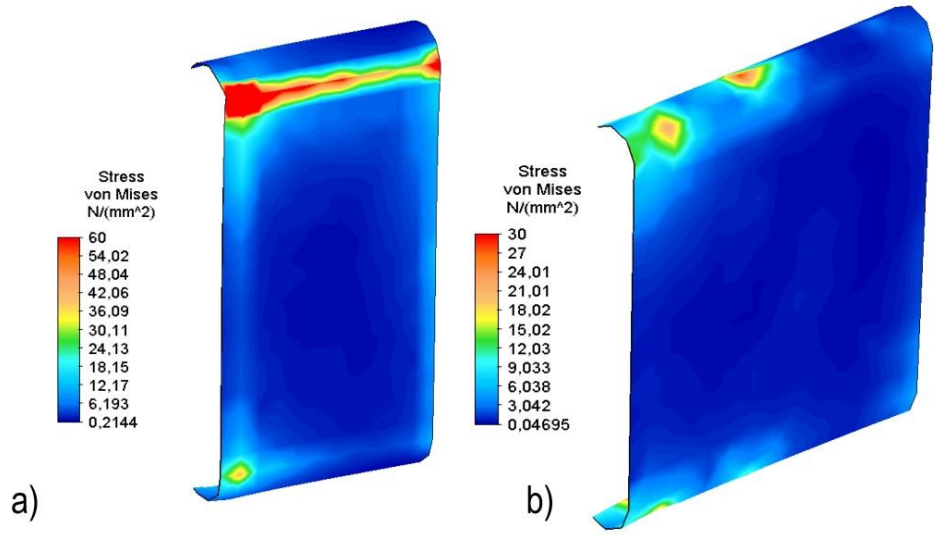

Fig. 12. Distribution of reduced stress in (a) 50 × 30 and (b) 50 × 50 mm glue lines

In the glue line of 50 × 50 mm joints, maximum contact pressures were equal to 30 N/mm^2 and reduced shear stress (Fig. 12). It should also be noted that the concentration of pressure between the mortise and tenon was located in front of the joint. This regularity reduced shear stress in the glue line and increased the strength of the joint. For these reasons, joints with longer tenons exhibit greater stiffness and strength.

CONCLUSIONS

This study was carried out to obtain background information concerning the moment resistance and stiffness of L-shaped and T-shaped round-end mortise and tenon furniture joints. The other purpose of this study was to perform numerical analysis of the joints by means of FEM. At the end of the study, the following conclusions were obtained:

1. Tenon width and tenon length both affected the moment resistance and stiffness of the joints.

2. Tenon length had a more significant effect on the moment resistance of the joints, while tenon width had a more significant effect on joint stiffness.
3. Ultimate moment resistances of individual joints were obtained when the front leg to side rail (L-shaped) joints were constructed with 50 mm depth by 50 mm length tenons, and back leg to side rail (T-shaped) joints were constructed with 40 mm depth by 50 mm length tenons.
4. Numerical analysis of the specimens as three-dimensional frame structures by finite element analysis (FEA) methods provided reasonable estimates consistent with the actual testing results.
5. Maximum stress in the glue line was concentrated at the edge and corners. In the middle point of the glue line, stresses had values close to zero. This leads to practical recommendations for assembly of furniture to take care of precise application of adhesive at the edges of the tenon.
6. Modeled joints had a shape-adhesive nature. This means that after exceeding the shear strains larger than the gap between the tenon and mortice, strengthening pressure between the mortise and tenon could be observed.

In conclusion, it can be said that the strength of a chair could be increased by considering these joint test results in the engineering design process.

ACKNOWLEDGEMENTS

This study was supported by Scientific and Technological Research Council of Turkey (TUBITAK) with the project number; 111O834, and Muğla Sıtkı Koçman University Scientific Research Project Office with the project number; 11/53.

REFERENCES CITED

ASTM D143-94 (2000). "Standard test methods for small clear specimens of timber," ASTM International, West Conshohocken, PA.

ASTM D 4442-92 (2001). "Standard test methods for direct moisture content measurement of wood and wood-base materials," ASTM International, West Conshohocken, PA.

Derikvand, M., and Ebrahimi, G. (2014). "Strength performance of mortise and loose-tenon furniture joints under uniaxial bending moment," *Journal of Forestry Research* 25(2), 483-486. DOI: 10.1007/s11676-014-0479-5.

Derikvand, M., and Eckelman, C. A. (2015). "Bending moment capacity of L-shaped mitered frame joints constructed of MDF and particleboard," *BioResources* 10(3), 5677-5690. DOI: 10.15376/biores.10.3.5677-5690.

Dzincic, I., and Skakic, D. (2012). "Influence of type of fit on strength and deformation of oval tenon-mortise joint," *Wood Research* 57(3), 469-477.

Dzincic, I., and Zivanic, D. (2014). "The influence of fit on the distribution of glue in oval tenon/mortise joint," *Wood Research* 59(2), 297-302.

Erdil, Y. Z., Kasal, A., and Eckelman, C. A. (2005). "Bending moment capacity of rectangular mortise and tenon furniture joints," *Forest Products Journal* 55(12), 209-213.

Gustafsson, S. I. (1995). "Furniture design by use of finite element method," *Holz als Roh-und Werkstoff* 53(4), 257-260.

Gustafsson, S. I. (1996). "Finite element modelling versus reality for birch chairs," *Holz als Roh-und Werkstoff* 54(5), 355-359. DOI: 10.1007/s001070050200.

Gustafsson, S. I. (1997). "Optimizing ash wood chairs," *Wood Science and Technology* 31(4), 291-301.

Hajdarević, S., and Martinović, S. (2014). "Effect of tenon length on flexibility of mortise and tenon joint," *Procedia Engineering* 69(2014), 678-685. DOI: 10.1016/j.proeng.2014.03.042.

Hajdarević, S., and Busuladžić, I. (2015). "Stiffness analysis of wood chair frame," *Procedia Engineering* 100(2015), 746-755. DOI:10.1016/j.proeng.2015.01.428.

Horman, I., Hajdarević, S., Martinović, S., and Vukas, N. (2010). "Numerical analysis of stress and strain in a wooden chair," *Drvna Industrija* 61(3), 151-158.

Horman, I., Hajdarevic, S., Vukas, N., Martinovic, S., and Sorn, S. (2012). "Effect of stretcher position on strength and stiffness of the chair side frame," *Technics Technologies Education Management* 7(2), 493-498.

Imirzi, H. Ö., Smardzewski, J., and Döngel, N. (2015). "Method for substitute modulus determination of furniture frame construction joints," *Turkish Journal of Agriculture and Forestry* 39(5), 775-785. DOI: 10.3906/tar-1406-92.

Kasal, A. (2004). *The Strength Performance of Sofa Frames Constructed of Solid Wood and Wood Composites*, PhD Dissertation, Institute of Science and Technology, Gazi University, Ankara, Turkey.

Kasal, B., and Pullela, S. V. (1995). *Development of Analytical Models for Furniture*. North Carolina State University, Furniture Manufacturing and Management Center, Raleigh, NC.

Kasal, A., Haviarova, E., Efe, H., Eckelman, C. A., and Erdil, Y. Z. (2013). "Effect of adhesive type and tenon size on bending moment capacity and rigidity of T-shaped furniture joints constructed of Turkish beech and Scots pine," *Wood and Fiber Science* 45(3), 287-293.

Kasal, A., Eckelman, C. A., Haviarova, E., Erdil, Y. Z., and Yalçın, İ. (2015a). "Bending moment capacities of L-shaped mortise and tenon joints under compression and tension loadings," *BioResources* 10(4), 7009-7020. DOI: 10.15376/biores.10.4.7009-7020

Kasal, A., Kuşkun, T., Efe, H., and Erdil, Y. Z. (2015b). "Relationship between static front to back loading capacity of whole chair and the strength of individual joints," in: *International Conference Research for Furniture Industry*, 17-18 September, Ankara, Turkey, p. 27.

Koç, K. H., Kizilkaya, K., Erdinler, E. S., and Korkut, D. S. (2011). "The use of finite element method in the furniture industry," *African Journal of Business Management*. 5(3), 855-865.

Kuşkun, T. (2013). *Effect of the Tenon Size and Loading Type on Chair Strength and Comparison of Actual Test and Finite Element Analyses Results*, Master of Science Thesis, Department of Woodworking and Industrial Engineering, Graduate School of Natural and Applied Sciences, Muğla Sıtkı Koçman University, Muğla, Turkey.

Likos, E., Haviarova, E., Eckelman, C. A., Erdil, Y. Z., and Özcifci, A. (2012). "Effect of tenon geometry, grain orientation, and shoulder on bending moment capacity and moment rotation characteristics of mortise and tenon joints," *Wood and Fiber Science* 44(4), 462-469.

Ratnasingam, J., Ioras, F., and McNulty, T. (2010). "Fatigue strength of mortise and tenon furniture joints made from oil palm lumber and some Malaysian timbers," *Journal of Applied Sciences* 10(22), 2869-2874.

Smardzewski, J. (1998). "Numerical analysis of furniture constructions," *Wood Science and Technology* 32(4), 273-286.

Smardzewski, J. (2002). "Strength of profile-adhesive joints," *Wood Science and Technology* 36(2), 173-183, PII 10.1007/s00226-001-0131-3.

Smardzewski, J., and Prekrat, S. (2009). "Optimisation of a sofa frame in the integrated cad-cae environment," *Electronic Journal of Polish Agricultural Universities* 12(4), 1.

Tankut, A. N., and Tankut, N. (2005). "The effects of joint forms (shape) and dimensions on the strengths of mortise and tenon joints," *Turkish Journal of Agriculture and Forestry* 29(6), 493-498.

Article submitted: May 12, 2016; Peer review completed: June 12, 2016; Revised version received: June 13, 2016; Accepted: June 14, 2016; Published: June 30, 2016.
DOI: 10.15376/biores.11.3.6836-6853